ISSN: 2229-6948(ONLINE)
DOI: 10.21917/ijct.2021.0368

TWELVE-PORT DUAL-POLARIZED DUAL-BAND MIMO ANTENNA FOR FIFTH-GENERATION MOBILE DEVICES

Jitendra Vaswani and Archana Agarwal
Department of Electronics and Communication Engineering, Sangam University, India

Abstract

This research article presents a twelve-port dual-band MIMO antenna for 5G and WLAN-enabled user equipment with dual-polarization characteristics. Both the operating frequencies are of sub-6GHz band centered at 3.6GHz and 5.5GHz respectively that are also independent of each other. Antenna polarizations depend on the excitation of the feed elements on the substrate. The antenna is designed using CST Studio Suite and fabricated on low-cost FR-4 substrate to ensure its easy availability and keep it cost-effective. The radiation pattern acquired for the proposed antenna is bi-directional with good gain and efficiency. The simulation results are in good covenant with experimental results.

Keywords:

5G, Dual-band, Dual-Polarized, MIMO, Slot Antenna

1. INTRODUCTION

Mobile communication and device-to-device communication systems are going to be revolutionized by the 5G because of its high-speed internet and device-to-device communication proposed in the 5G specifications. Since the launch of 3G, the hunger and expectations for high-speed internet are increasing and life with high-speed internet is being felt like living in ancient times. A good antenna is a must for any high-speed communication system. The researchers are designing the antennas to quench the requirements of the same. MIMO antennas have been the key to get increased speed in wireless communication systems. A two-element antenna prototype was proposed in [1] and this research paper discusses the 12 element antenna systems for 5G smartphones.

A good number of papers have been communicated by the researchers and a few of those are being discussed here. In 2011, a researcher proposed a multi-frequency antenna that was miniaturized and operated on 2.5/3.5/5.5-GHz bands. It had good radiation patterns and sufficient gains across the proposed bands of antenna operation [2]. An eight-element antenna array based on capacitive coupling elements PIFA was proposed in the year 2014. The structure had the highest mutual coupling of -10 dB and hence proposed the proposed as a good candidate for MIMO antenna and for implementing diversity in mobile terminals [3]. A circularly polarized antenna for 5G mobile system is proposed and has achieved around 45% reduction in conventional patch size [4]

An eight-element MIMO antenna system for 5th Generation wi-fi system was discussed that operates on 5GHz band, the design was verified on using two different software platforms i.e. ADS momentum and CST Studio to compare the performance of MoM and FDTD which are different modeling techniques [5]. An array of 8 dual-polarized hybrid antennas that operated in the 2.6-GHz band was also considered for 5G communication systems [6]. A hybrid antenna system with 8 elements covering the 3.6GHz band of 5G communication system was proposed that had a good gain, efficiency, and ECC was presented in 2016. It proposed a 2-elements system for 4G communication and an 8-element system for 5G devices to quench the demands of 5G [7]. A dual-band four-element SRR-loaded structure with an inverted L-monopole antenna was proposed. Its operating bands were around 2.9GHz and 5.68GHz in the sub-6GHz band of 5G communication. The realized gain was around 4dB and the value of ECC was less than 0.05 in the antenna band of operation [8].

Another 8-element loop antenna design was presented in [9], wherein the antenna was proposed on smartphone frame and proposed the isolation of more than 10dB is acceptable isolation. Another SRR-loaded design was proposed in [10] for 5G communication systems, in which the bandwidth of the antenna was extended by merging the narrow bands. Other works on sub-6GHz band of 5G are discussed in [11]-[15]. A self–decoupling structure of MIMO antennas was discussed that operates in the 3.5GHz band and has good gain [16]. A four-port multi-band antenna was proposed in which each of the four elements was sited at each corner of the substrate and a gain of around 2 dB was achieved. Further, a design is proposed with 8 elements on the same substrate [17].

Most of the previous designs were single-band, limited to not more than 8 ports and the dimensions of the antenna were almost 1.25 times the dimensions of the antenna proposed in this paper. A basic design was simulated and discussed in [18], in which 4 antennas were placed at four corners of the substrate. The results obtained in previous work encouraged the design of a twelve-port antenna for a 5G mobile device with a screen size of nearly 5 inches. This paper presents 12 ports antenna that operates on a sub-6GHz band of 5G and a 5.5GHz band for WLAN communication. The design of the slots is kept identical while repeating the antenna structure for achieving 12 ports on a single substrate. The prototype is designed, fabricated and laboratory measurement results are obtained for the same.

2. ANTENNA DESIGN

In previous work, a two-port antenna, the basic antenna design was proposed and shown in **Error! Reference source not found.**(a) and **Error! Reference source not found.**(b) [1]. Based on the same, a 12 port MIMO antenna system prototype is proposed for smartphones in this paper as shown in **Error! Reference source not found.**(c). The antenna system is designed on a low-cost FR-4 substrate with a dielectric constant $\varepsilon_r = 4.4$ and loss tangent $\tan\delta = 0.002$. The dimensions of the substrate are 120mm×60mm×1.6mm. The 12 antennas elements can be categorized into two sets of antennas. The first set comprising of eight antenna elements symmetrically placed at four corners of the substrate and the second set having four antenna elements positioned along the longer edges of the substrate, two on each

side amid the antennas placed at the corners. Each of the antenna element is fed by a 50-ohm microstrip transmission line as shown in **Error! Reference source not found.**(c), there are square ring slots etched into the ground plane that is responsible for the resonant frequencies of the antenna. The dimensions and position of the slots are optimized to get the desired resonant frequencies. The resonant frequency of the antenna is proportional to slot length 0.5(*a*+*s*). The outer slot of length 14 mm is responsible for the 3.6GHz band and the inner slot of 9.6 mm is responsible for the 5.5GHz band. The width of each slot is 0.375 mm and is denoted by *s*.

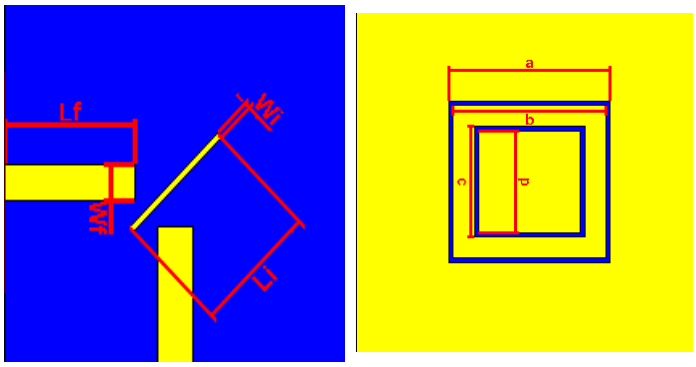

(a) (b)

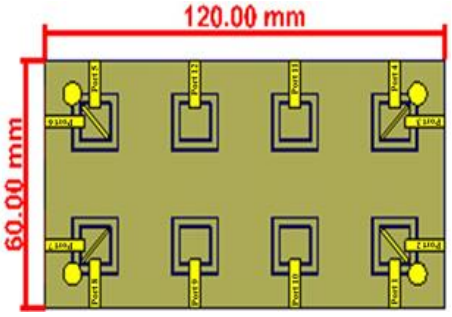

(c)

Fig.1(a) Front view of the proposed slot antenna Unit Cell (b) Back view of the proposed slot antenna Unit Cell (c) Transparent View of Proposed 12 Port Antenna

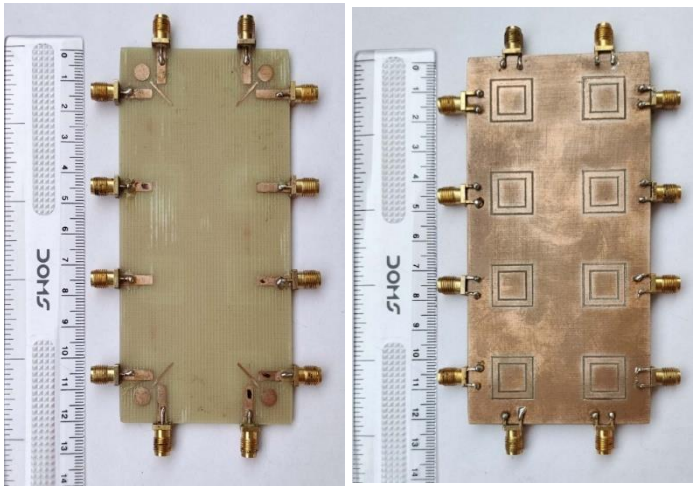

(a) (b)

Fig.1. (a) Front View of the Fabricated Antenna (b) Back View of the Fabricated Antenna

Table.1 Optimized Design Parameters Values

Parameter	Value (mm)
a	14
b	13.75
c	9.6
d	8.85
h	1.6
L_f	11.75
L_i	11
S	0.375
W_f	3
W_i	0.5

The antenna is fabricated on FR-4 substrate for testing. The front and back of the antenna are shown in Fig.1(a) and Fig.1(b) respectively. All twelve connectors are soldered for testing purposes. The setup for testing of the proposed antenna for s-parameter measurements on Vector Network analyzer in antenna testing lab is shown in Fig.2. The Keysight PNA-L Microwave Network Analyser, model number N5234A is used that can do measurements up to the frequency of 43.5GHz.

Fig.2. Experimental Setup for S parameter measurement

3. RESULTS AND DISCUSSIONS

The results discussed in this paper are both simulations as well as measured results. Firstly, the simulated S-parameter results are shown in Fig.3 for port 1, port 2, and port 9. The results for only three port are shown in the paper as Port 1, Port 4, Port 5, and Port 8 are identical, Port 2, Port 3, Port 6, and Port 7 are identical and Port 9 to Port 12 are identical due to their symmetrical position on the substrate. The first resonant frequency for antenna 1 is 3.6GHz with a bandwidth of 400MHz approx. and second, the resonant frequency is 5.45GHz with a bandwidth of 600MHz. Similarly, the first resonant frequency for antenna 2 is 3.6GHz with a bandwidth of 400MHz approx. and second, the resonant frequency is 5.5GHz with a bandwidth of 675MHz, and the first resonant frequency for antenna 9 is 3.6GHz with a bandwidth of 400MHz approx. and second, the resonant frequency is 5.5GHz with a bandwidth of 600MHz approx.

The results of Antenna 1, Antenna 4, Antenna 5, and Antenna 8 are identical because of their dimensions and positions and similarly Antenna 2, Antenna 3, Antenna 6, and Antenna 7 and for Antenna 9, Antenna 10, Antenna 11, and Antenna 12 are identical for the alike reasons.

The comparison of simulated and experimental results for the proposed antenna design is shown in Fig.4 for port 1, port 2, and port 9. It can be verified that the first resonant frequency is at 3.6GHz for all ports and the second resonant frequency between 5.5 to 6GHz. The shift in second resonant frequency may be due to variation of the dimension of the inner slot during antenna fabrication which can be improved by getting a more accurately fabricated antenna.

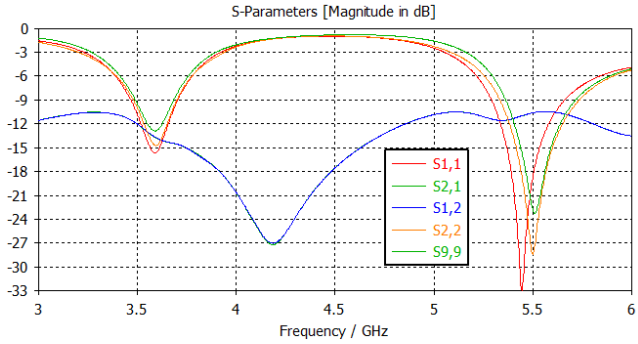

Fig.3. Simulated S-Parameter Results for Port 1, Port 2, and Port 9

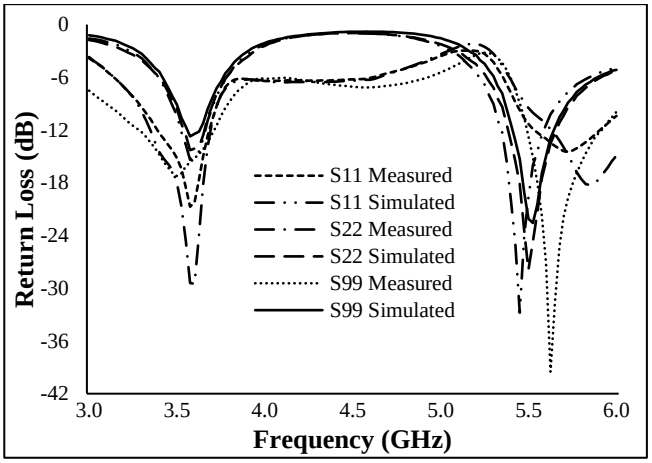

Fig.4. Simulated and Measured S11 Results for Port 1, Port 2, and Port 9

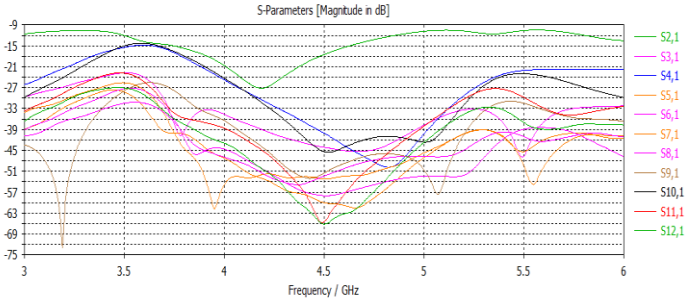

Fig.5. Mutual Coupling of Port 1 with all other Ports

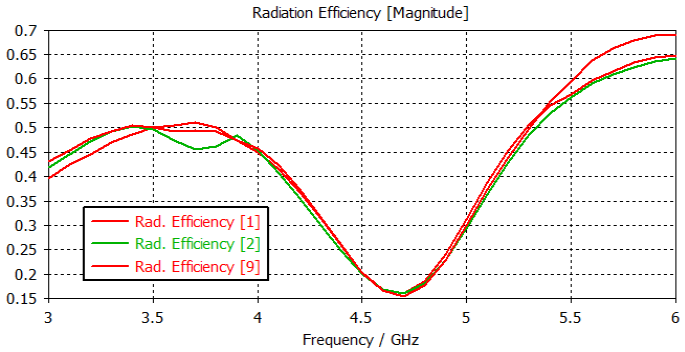

Fig.6. Radiation Efficiency of Antenna Port 1, Port 2, and Port 9

Table.2. Antenna Radiation Efficiency at Different Bands

Antenna Port	Radiation Efficiency in 3.6GHz Band		Radiation Efficiency in 5.5GHz Band	
	Min. Value	Max. Value	Min. Value	Max. Value
1	49%	51%	46%	63%
2	50%	51%	44%	62%
3	50%	51%	44%	62%
4	49%	51%	46%	63%
5	49%	51%	46%	63%
6	50%	51%	44%	62%
7	50%	51%	44%	62%
8	49%	51%	46%	63%
9	49%	50%	45%	68%
10	49%	50%	45%	68%
11	49%	50%	45%	68%
12	49%	50%	45%	68%

The radiation efficiency of antenna port 1, port 2, and port 9 are shown in Fig.6. It is around 50% in the 3.6GHz band and around 60% in the 5.5GHz band of operation. Table.2 shows the maximum and minimum values of radiation efficiencies for all 12 antenna elements.

The isolation between antenna port 1 and port 2 is more than 10 dB as shown in Fig.5. The maximum mutual coupling is between antenna 1 and antenna 2 and similar pairs namely 3 and 4, 5, and 6 and 7 and 8, so the results of port 1 are shown here. The coupling between antennas was reduced by using parasitic patches, that act as isolation between the antennas. One circular and the other is a thin rectangular patch placed between the feed elements of the antenna system as shown in **Error! Reference source not found.**. The circular patch reduced the mutual coupling for the above-mentioned antenna pairs for the 3.6GHz frequency band and the thin rectangular patch served the same purpose for the 5.5GHz band. The S-parameter with and without parasitic patches is also shown in Fig.7. The mutual coupling between the antennas in the proposed design is also less than -10 dB for all antennas.

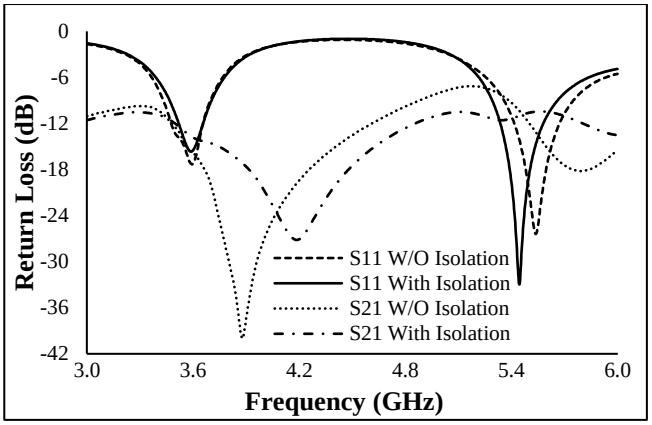

Fig.7. S Parameters for Port 1, With and Without Isolation

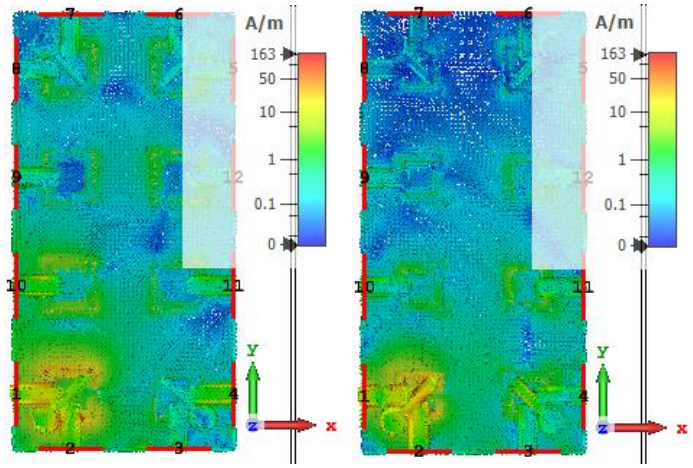

(a) (b)

Fig.8. (a) Surface Current Distribution at 3.6GHz for port 1 on the complete antenna (b) Surface Current Distribution at 5.5GHz for port 1 on complete antenna

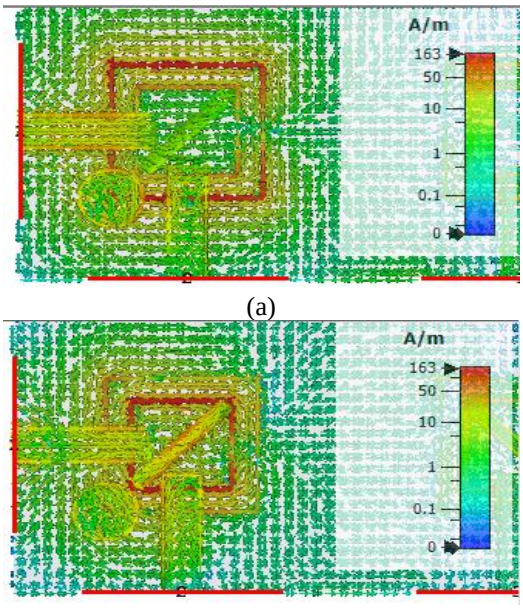

(a)

(b)

Fig.9. (a) Current Distribution at 3.6GHz for port 1 (b) Current Distribution at 5.5GHz for port 1

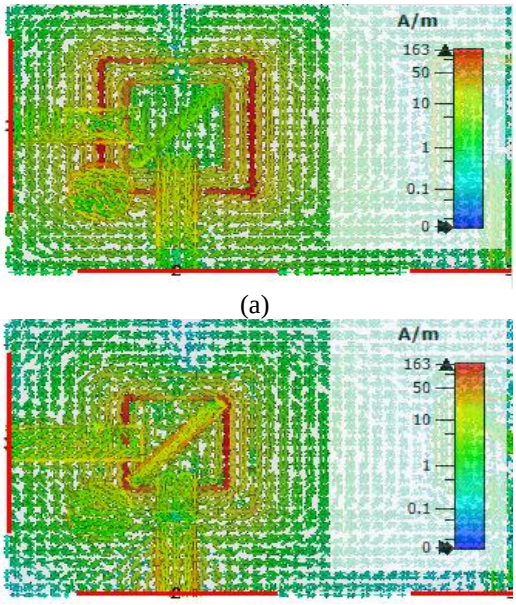

(a)

(b)

Fig.10. (a) Current Distribution at 3.6GHz for port 2 (b) Current Distribution at 5.5GHz for port 2

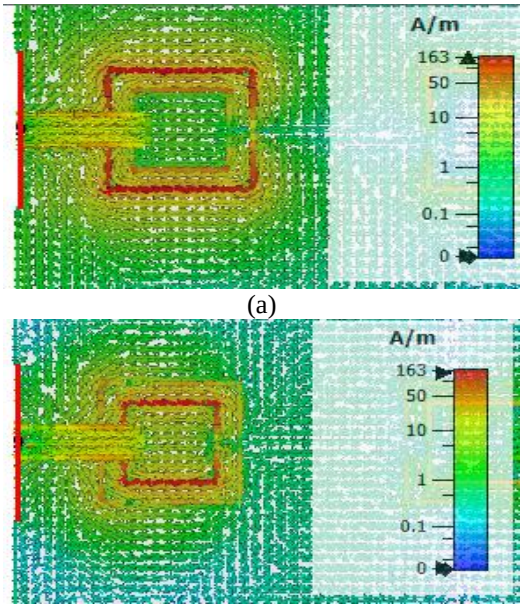

(a)

(b)

Fig.11. (a) Current Distribution at 3.6GHz for port 9 (b) Current Distribution at 5.5GHz for port 9

The Fig.8(a) and Fig.8(b) shows the surface current distribution on the complete antenna for port 1 at both frequencies under consideration. Surface current distribution for port 1, port 2, and port 9, when excited individually is shown in Fig.9-Fig.11.

The Fig.9(a)-Fig.11(a) show high current density is observed in the outer slot at 3.6GHz validating that the outer slot is responsible for lower operating frequency. Similarly, it can be seen from Fig.9(b)-Fig.11(b) that the inner slot is responsible for the higher operating frequency band of 5.5GHz. Further, Fig.9-Fig.11 show a high current density is around the circular parasitic patch at 3.6GHz and linear patch at 5.5GHz frequency

demonstrating the role of patches to improve the isolation at lower and higher frequencies respectively.

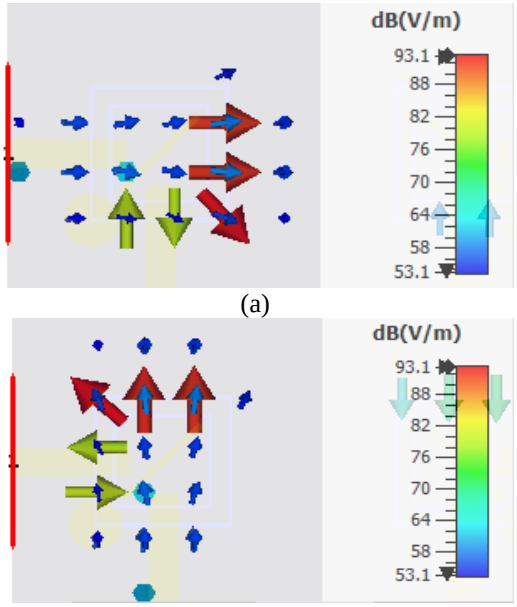

(a)

(b)

Fig.12. (a) Electric Field for Port 1 at 3.6GHz (b) Electric Field for Port 2 at 3.6GHz

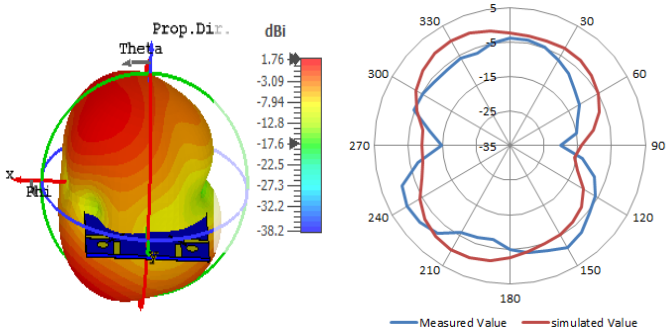

(a) (b)

Fig.13. (a) 3D Radiation Pattern for Antenna Port 1 at 3.6GHz (b) Simulated v/s Normalized Measured 2D Radiation for Port 1 at 3.6GHz

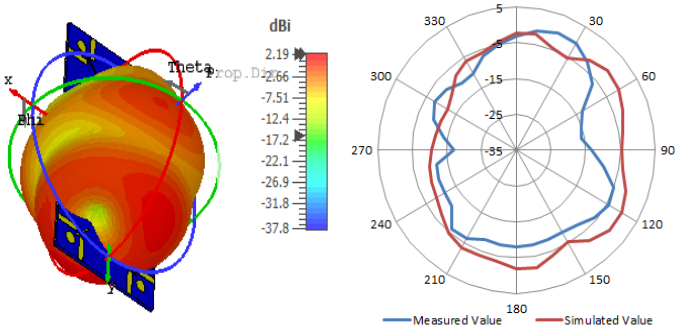

(a) (b)

Fig.14. (a) 3D Radiation Pattern for Antenna Port 2 at 3.6GHz, (b) Simulated v/s Normalized Measured 2D Radiation for Port 2 at 3.6GHz

The Fig.12 shows the orientation of the electric field when port 1 and port 2 are excited respectively. It can be seen from the Figure that the orientation of the field is perpendicular to each other, thus verifying the dual-polarization characteristic of the antenna.

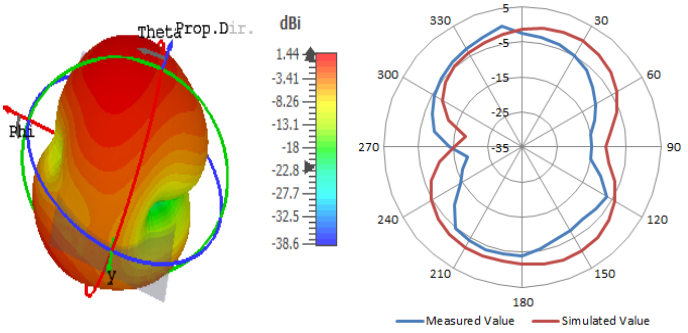

(a) (b)

Fig.15. (a) 3D Radiation Pattern for Antenna Port 9 at 3.6GHz, (b) Simulated v/s Normalized Measured 2D Radiation for Port 9 at 3.6GHz

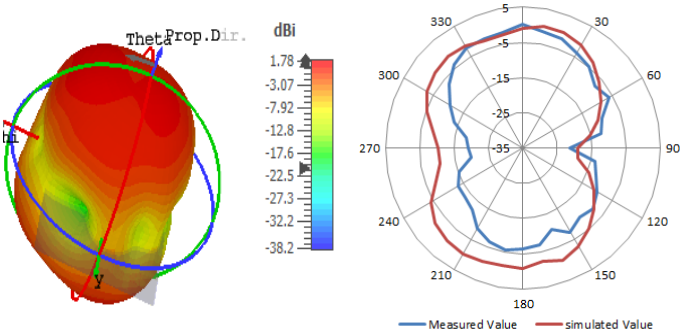

(a) (b)

Fig.16. (a) 3D Radiation Pattern for Antenna Port 1 at 5.5GHz (b) Simulated v/s Normalized Measured 2D Radiation for Port 1 at 5.5GHz

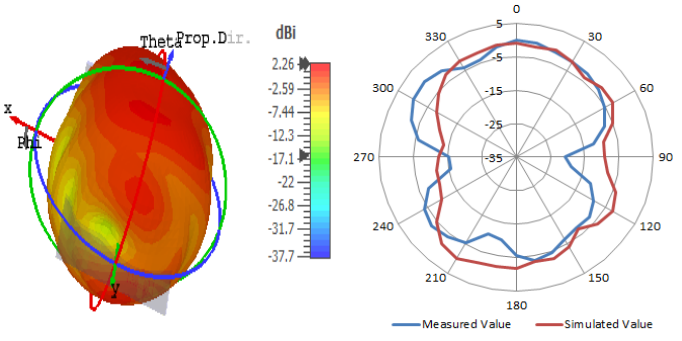

(a) (b)

Fig.17. (a) 3D Radiation Pattern for Antenna Port 2 at 5.5GHz, (b) Simulated v/s Normalized Measured 2D Radiation for Port 2 at 5.5GHz

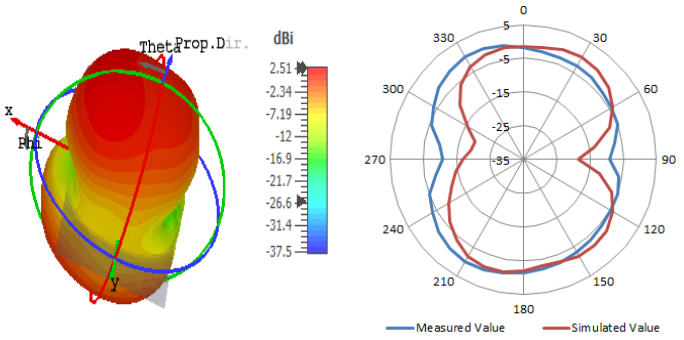

(a) (b)

Fig.18. (a) 3D Radiation Pattern for Antenna Port 9 at 5.5GHz, (b) Simulated v/s Normalized Measured 2D Radiation for Port 9 at 5.5GHz

Table.3. Antenna Gain at Different Operating Frequencies

Antenna	Gain at 3.6GHz	Gain at 5.5GHz
1	1.76	1.78
2	2.19	2.26
3	2.19	2.26
4	1.76	1.78
5	1.76	1.78
6	2.19	2.26
7	2.19	2.26
8	1.76	1.78
9	1.44	2.51
10	1.44	2.51
11	1.44	2.51
12	1.44	2.51

The simulated gain for the antenna ranges from 1.44 dB to 2.19 dB at 3.6GHz and 1.78 dB to 2.51 dB for 5.5GHz as shown in

Table.3. 3D radiation pattern and Simulated v/s Normalized Measured 2D Radiation pattern are shown from Fig.13 to Fig.18 for port 1, port 2 and port 9 at 3.6GHz and 5.5GHz respectively. It can be seen from the above-mentioned Figure, that the antenna radiation pattern is bi-directional. The anechoic chamber measurements for antenna port 1 at 3.6GHz are compared with simulated values as shown in Fig.13(b), which shows the agreement amid the simulated and measured results. Similarly, the measurements at 5.5GHz for port 1 are shown in Fig.14(b) are well in agreement with the simulated results. Similar agreement amid simulated and measured results is observed from Fig.15(b) to Fig.18(b). The Fig.19 depicts the variation of antenna gain for port 1, port 2, and port 9 with variation in the operating frequency of the antenna.

The envelope correlation coefficient is shown in Fig.20 for antenna 1 and antenna 2 is well below 0.01 in 3.4GHz to 4GHz and for 5.2GHz to 5.6GHz, then it rises to 0.08 for 5.8GHz. The emphasis is more on port 1 and port 2, as the mutual coupling amid these two ports, is high as compared to any other combination of port 1 or port 2. For any other antenna pair, it is well below the threshold limit of 0.5. The diversity gain for various port combinations is around 10 dB in the 3.6GHz band and more than 9.7 dB in the 5.5GHz band as shown in Fig.21.

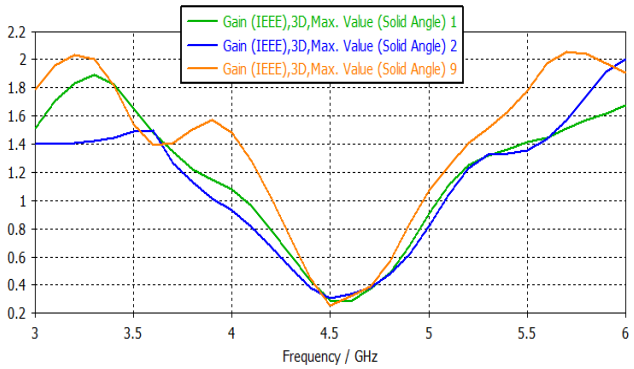

Fig.19. Variation of Antenna Gain for Port 1, Port 2, and Port 9 with Frequency

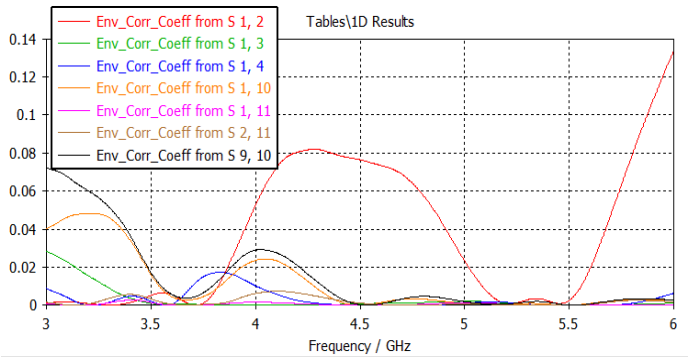

Fig.20. Envelope Correlation Coefficient for Various Combinations of Antenna Ports

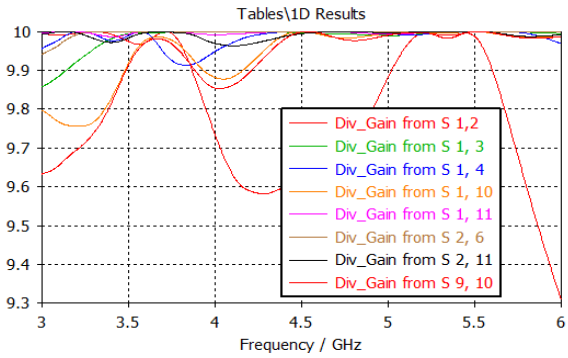

Fig.21. Diversity Gain from S-parameter for Various Port Combinations

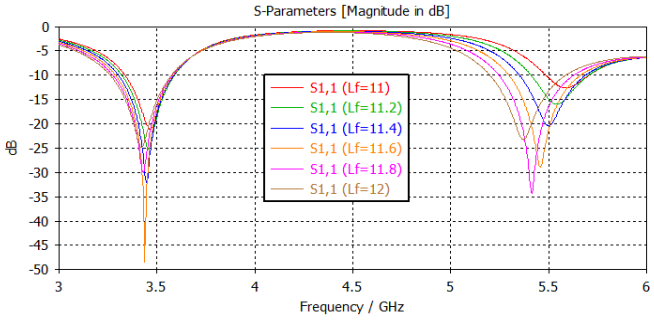

Fig.22. Effect of Variation of Length of Feed-line on S11

The length of feed-lines was varied from 11 mm to 12 mm and its effect was observed primarily on impedance matching characteristics as shown in Fig.22 and Fig.23. It was observed that the S11 value was shifting between 3.6GHz and 5.5GHz. For smaller values of L_f, return loss for 3.6GHz was better and not that good for 5.5GHz. As the length was increased, the return loss improved for the 5.5GHz band but simultaneously it started getting less negative for 3.6GHz. An increase in bandwidth for the 5.5GHz band was also observed with increased feed-line length. Also, for a length greater than 11.75 mm, the resonant frequency gets shifted to a lower frequency band. Similar characteristics were observed for antenna 2 and antenna 10. Also, the isolation between antennae 1 and 2 was decreasing with increasing the feed-lines. Considering all the above-mentioned points, the length of the feed-line was kept to be 11.75 mm.

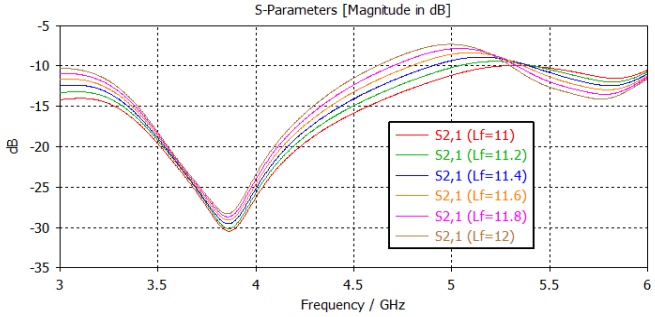

Fig.23. Effect of Variation of Length of Feed-line on S21

The Table.4 presents the comparison of fundamental properties of 5G antennas reported in the literature from [2] to [17] with the proposed 5G antenna. It shows the antenna's performance is at par with the reported antennas in terms of bandwidth, gain, efficiency, overall size, isolation and ECC. Further, the proposed design has ample space for the placement of other components of mobile user equipment, which is not considered in the reported literature.

Table.4. Comparison between reported and proposed 5G antennas

Method	Port	Band-width (GHz)	Gain (dBi)	Effic-iency (%)	Overall Size (mm^2)	Isolation (dB)	ECC
[2]	1	2.4-2.7 3.1-4.15 4.93-5.89	1.85 2.19 2.57	NA	38×25	NA	NA
[6]	8	2.55-2.65	NA	55–63	68×136	18	<0.15
[7]	8	3.4-3.6	2.5	62–78	70×130	10	<0.2
[10]	4	3.1-3.2 3.6-4.0	1.79 2.39	58–67	60×60	20 17	<0.1
[17]	4	2.5-2.8 3.4-4.0 4.9-5.7	2–3	64–75 73–76 69–75	75×150	17	<0.05
Proposed	12	3.4-3.8 5.3-5.9	1.4-2.2 1.8-2.5	49–51 44–68	60×120	11	<0.06 <0.09

4. CONCLUSION

In this paper, a twelve-element dual-band MIMO antenna having dual-polarization that operates in a sub-6GHz band of 5G technology is presented. The polarization of the antenna depends on the excitation of the feed elements and hence on the position of feeds on the substrate. The dimensions of the FR-4 substrate are chosen to match the size of the user equipment of 5G. Both operating frequencies 3.6GHz and 5.5GHz can be varied independently, without affecting the other. The proposed antenna has good gain, efficiency, sufficient isolation, and the simulation results are backed by the lab measurements for s-parameter and radiation pattern. The antenna is proposed and fabricated on FR-4 the substrate to clinch its easy availability and its cost-effectiveness. The antenna has good performance in terms of ECC less than 0.1 and high diversity gain greater than 9.7dB.

In future work, the measurements for Co and Cross fields will be reported to verify the polarization characteristics of the antenna. The efficiency and gain of the antenna need to be improved as a part of future work.

REFERENCES

[1] J. Vaswani and A. Agarwal, "Dual-Band, Dual-Polarized Two Element Slot Antenna for Fifth Generation Mobile Devices", *Turkish Journal of Computer and Mathematics Education*, Vol. 12, No. 3, pp. 4822-4830, 2021.

[2] Jing Pei, An-Guo Wang, Shun Gao and Wen Leng, "Miniaturized Triple-Band Antenna with a Defected Ground Plane for WLAN/WiMAX Applications", *IEEE Antennas Wireless Propagations Letters*, Vol. 10, pp. 298-301, 2011.

[3] A.A. Al-Hadi, J. Ilvonen, R. Valkonen and V. Viikari, "Eight-Element Antenna Array for Diversity and Mimo Mobile Terminal in LTE 3500 MHz Band", *Microwave and Optical Technology Letters*, Vol. 56, No. 6, pp. 1323-1327, 2014.

[4] Ka Ming Mak, Hau Wah Lai, Kwai Man Luk and Chi Hou Chan, "Circularly Polarized Patch Antenna for Future 5G Mobile Phones", *IEEE Access*, Vol. 2, pp. 1521-1529, 2014.

[5] S.A. Nasir, M. Mustaqim and B.A. Khawaja, "Antenna Array for 5th Generation 802.11AC Wi-Fi Applications", *Proceedings of 11th Annual High Capacity Optical Networks and Emerging/Enabling Technologies (Photonics for Energy)*, pp. 20-24, 2014.

[6] M.Y. Li, "Eight-Port Orthogonally Dual-Polarized Antenna Array for 5G Smartphone Applications", *IEEE Transactions on Antennas and Propagation*, Vol. 64, No. 9, pp. 3820-3830, 2016.

[7] Y. Ban, C. Li, C. Sim, G. Wu and K.L. Wong, "4G/5G Multiple Antennas for Future Multi-Mode Smartphone Applications", *IEEE Access*, Vol. 4, pp. 2981-2988, 2016.

[8] D. Sarkar and K.V. Srivastava, "Compact Four-Element SRR-Loaded Dual-Band MIMO Antenna for WLAN/WiMAX/WiFi/4G-LTE and 5G Applications", *Electronics Letters*, Vol. 53, No. 25, pp. 1623-1624, 2017.

[9] H. Wang and G. Yang, "Compact and Low-Profile Eight-Element Loop Antenna Array for the 3.6-Ghz MIMO Operation in the Future Smartphone Applications", *Proceedings of 6th Asia-Pacific Conference on Antennas and Propagation*, pp. 1-3, 2017.

[10] D. Sarkar and K.V. Srivastava, "Four Element Dual-band Sub-6 GHz 5G MIMO Antenna using SRR-loaded Slot-Loops", *Proceedings of IEEE International Conference on*

Electrical, Electronics and Computer Engineering, pp. 1-5, 2015.

[11] X. Zhao, S.P. Yeo, and L.C. Ong, "Decoupling of Inverted-F Antennas with High-Order Modes of Ground Plane for 5G Mobile MIMO Platform", *IEEE Antennas Wireless Propagations Letters*, Vol. 66, No. 9, pp. 4485-4495, 2018.

[12] A. Alieldin, "A Triple-Band Dual-Polarized Indoor Base Station Antenna for 2G, 3G, 4G and Sub-6 GHz 5G Applications", *IEEE Access*, Vol. 6, pp. 49209-49216, 2018.

[13] Y. Li, C. Sim, Y. Luo and G. Yang, "12-Port 5G Massive MIMO Antenna Array in Sub-6GHz Mobile Handset for LTE Bands 42/43/46 Applications", *IEEE Access*, Vol. 6, pp. 344-354, 2018.

[14] W. Hu, "Dual-Band Eight-Element MIMO Array using Multi-Slot Decoupling Technique for 5G Terminals", *IEEE Access*, Vol. 7, pp. 153910-153920, 2019.

[15] N. Ferdous, G. Chin Hock, H.A.S. Hamid, M.N.A. Raman, T. Sieh Kiong and M. Ismail, "Design of a Small Patch Antenna at 3.5 GHZ for 5G Application", *Proceedings of IOP Conference Series: Earth and Environmental Science*, Vol. 268, No. 1, pp. 1-15, 2019.

[16] Z. Ren, A. Zhao and S. Wu, "MIMO Antenna with Compact Decoupled Antenna Pairs for 5G Mobile Terminals", *IEEE Antennas and Wireless Propagation Letters*, Vol. 18, No. 7, pp. 1367-1371, 2019.

[17] N.O. Parchin, H.J. Basherlou, Y.I.A. Al-Yasir and A. Ullah, "Multi-Band MIMO Antenna Design with User-Impact Investigation for 4G and 5G Mobile Terminals", *Sensors*, Vol. 19, No. 3, pp. 1-16, 2019.

[18] J. Vaswani and A. Agarwal, "A Four Port, Dual Band Antenna for Fifth Generation Mobile Communication and WLAN Services", *ACTA Techinca Corviniensis - Bulletin of Engineering*, Vol. 4, No. 13, pp. 73-76, 2020.